Eur. Phys. J. B (2013) 86: 21
DOI: 10.1140/epjb/e2012-30748-y

THE EUROPEAN PHYSICAL JOURNAL B

Regular Article

On the correlation between supercooling, superheating and kinetic arrest in a magnetic glass $Pr_{0.5}Ca_{0.5}Mn_{0.975}Al_{0.025}O_3$

Kaustav Mukherjee[a,b], Kranti Kumar, Alok Banerjee, and Praveen Chaddah

UGC-DAE Consortium for Scientific Research, University Campus, Khandwa Road, Indore-452001, M.P, India

Received 15 August 2012 / Received in final form 10 October 2012
Published online 23 January 2013 –

Abstract. We report a quantitative investigation of the magnetic field-temperature phase diagram by taking into account a simple phenomenological model arising out of the interplay of kinetic arrest and thermodynamic transitions in a magnetic glass $Pr_{0.5}Ca_{0.5}Mn_{0.975}Al_{0.025}O_3$, through magnetization measurements. Such studies are necessary as kinetic arrest plays an important role in the formation of "magnetic glasses", which has been observed in systems undergoing first order magnetic phase transitions. It has been shown that disorder in a system results in the formation kinetic arrest (H_K,T_K) band, like supercooling (H^*,T^*) and superheating (H^{**},T^{**}) band. Quantitative proofs are given to show that (H_K,T_K) band is anticorrelated with (H^*,T^*) and (H^{**},T^{**}) bands, while the later two are correlated among themselves. Analysis of time dependence of magnetization at different temperatures is carried out to establish the fact that the kinetic arrested state is different from the supercooled state.

1 Introduction

In the recent context of research in manganites and magnetocaloric materials, a completely new type of glassy behavior has been discovered in systems undergoing first order magnetic phase transitions [1–12]. Such type of glassy behavior has also been observed in other oxides, like $LuFe_2O_4$, at low temperatures [13]. In striking contrast with spin glass [14,15] this 'magnetic glassy' state arises out of a kinetically arrested first-order ferromagnetic (FM) to antiferromagnetic (AF) (or vice versa) phase transition. It is also to be noted that the characteristics observed for this magnetic glasses are different from those observed from spin/reentrant spin glasses [15]. 'Kinetic arrest' implies a viscous retardation of growth of the low temperature phase out of the supercooled high temperature phase. Such an arrest of kinetics also inhibits a first order phase transition (FOPT) where both the phases on either side of the transition, have long range structural and magnetic order. The high temperature phase persists in the low temperature region, where it is energetically unstable and 'lack of dynamics triumphs over thermodynamics'. Moreover, the fraction of glass-like arrested state at low temperature can be tuned at the cost of the coexisting equilibrium phase of contrasting order. Thus it can be said that in the formation of magnetic glasses interplay of supercooling, superheating and kinetic arrest plays an important role in its formation. Hence a detailed investigation of the association among kinetic arrest and thermodynamics transitions is required.

In this context, it is to be noted that a general phenomenon associated with FOPT is the presence of hysteresis in cycling through transition, as temperature (T) or magnetic field (H) is decreased or increased and is believed to be associated with supercooling and superheating, respectively [16]. Presence of disorder in samples would result in broadening of transition with a spatial distribution of phase transition (H_N,T_N) line across the sample [17]. Hence, a presence of large number of (H_N,T_N) lines across the sample would result in formation of band. The spinodal lines corresponding to the limit of supercooling (H^*,T^*) and superheating (H^{**},T^{**}) would be broadened into bands for samples with quenched disorder [18]. Moreover, such broadening of (H^*,T^*) and (H^{**},T^{**}) bands is consistent with the Landau theory of phase transitions. However, for glass-like freezing of supercooled liquid a clear (H_K,T_K) band is not defined. Moreover, even though the origin and important role played by the kinetic arrest is highlighted in literature, quantitative tracing of it in form of the band is lacking in literature.

Hence in this article, for the first time we present: (i) a quantitative proof that disorder in a system results in the formation of (H_K,T_K) band, (ii) the heuristic phase diagrams proposed earlier [2,4], i.e. (H_K,T_K) band is anticorrelated with (H^*,T^*) and (H^{**},T^{**}), while the later two are correlated among themselves has been quantitatively verified, and (iii) through quantitative analysis of time decay measurements it is proved that the supercooled phase is different from the kinetic arrest phase. All these investigations were carried out on $Pr_{0.5}Ca_{0.5}Mn_{0.975}Al_{0.025}O_3$ through magnetization measurements. This compound is chosen as there is coexisting fractions of equilibrium

[a] e-mail: kmpersonal2@gmail.com
[b] *Present address*: Graduate School of Engineering Science, Osaka University, Osaka 560-8531, Japan.

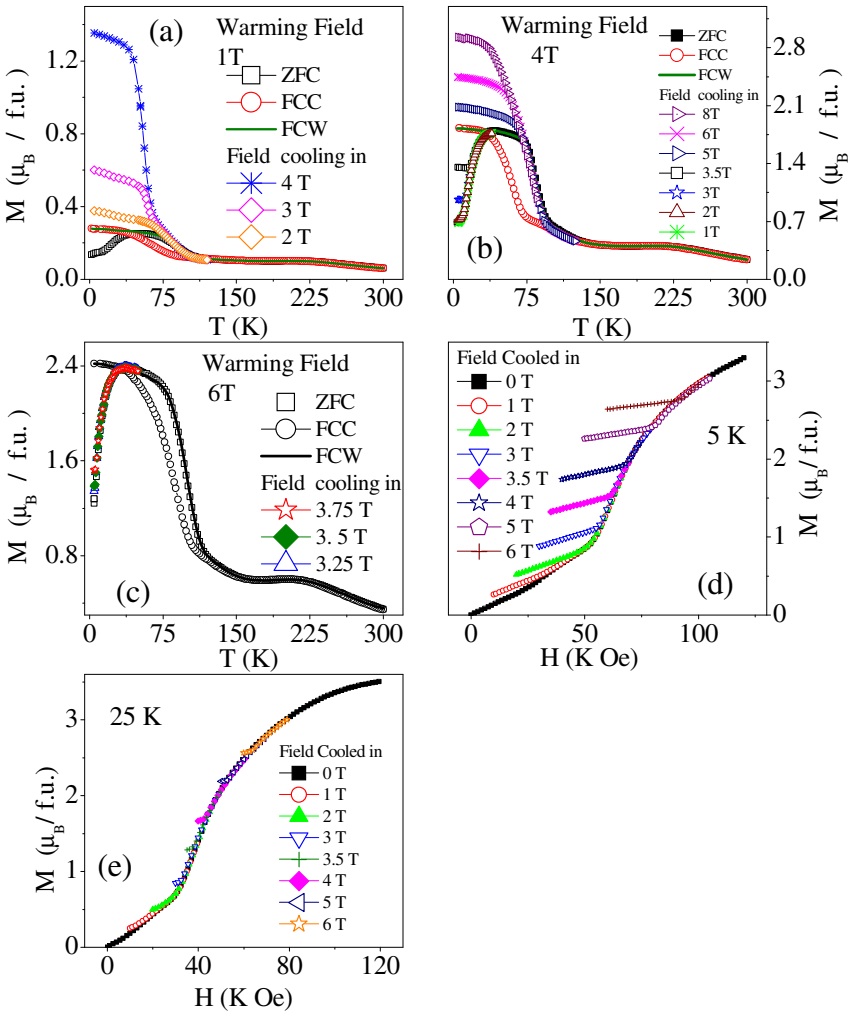

Fig. 1. (Color online) Field annealing M-T curves along with ZFC, FCC, FCW curves at (a) 1 Tesla, (b) 4 Tesla, and (c) 6 Tesla for the compound $Pr_{0.5}Ca_{0.5}Mn_{0.975}Al_{0.025}O_3$. The field annealing graphs were obtained while heating in the indicated warming field after cooling the compound from 320 K to 5 K in various cooling fields. Field annealing M-H curves at (d) 5 K and (e) 25 K. The curves were obtained after cooling the compound in different cooling fields to the measurement temperatures and then increasing the field from cooling field values.

ferromagnetic metallic phase and arrested antiferromagnetic insulating phases at low temperatures [4].

2 Experimental details

The compound $Pr_{0.5}Ca_{0.5}Mn_{0.975}Al_{0.025}O_3$ is the same as that used in reference [4]. The magnetization measurements are performed by using a commercial 14 Tesla PPMS-Vibrating compound Magnetometer system from Quantum Design.

3 Results and discussions

3.1 DC Magnetization studies through distinctive CHUF (cooling heating in unequal fields) protocol

Deliberate substitution of 2.5% Al on Mn site in robust charge-ordered $Pr_{0.5}Ca_{0.5}MnO_3$ results in field history dependent coexisting fractions of equilibrium FM metallic (FM-M) and arrested AF insulating (AF-I) phases [4]. This is due to the fact that a hindered FOPT gives rise to a glass-like kinetically arrested AF-I phase fraction at low temperatures which depends on the magnetic field and can convert to the equilibrium FM-M phase. Hence, to methodically investigate the nature of the coexisting phases in this compound, field annealing protocols are carried out. The field annealing protocols involve cooling the compound from room temperature in one cooling field (H_c) and heating the compound in another warming field (H_w). This cooling and heating in unequal fields has been referred as the CHUF protocol [10,11]. Figures 1a, 1b and 1c show the temperature response of zero field cooled (ZFC), field cooled cooling (FCC) and field cooled warming (FCW) magnetization (M) at fields 1, 4 and 6 Tesla, along with magnetization versus temperature curves while heating, at the warming field, after cooling the compound from 320 to 5 K at different cooling field. For all cases

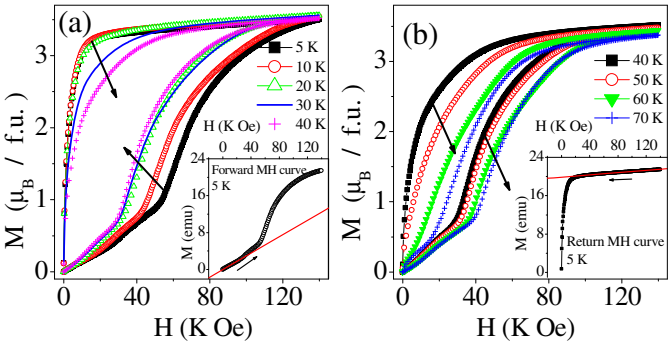

Fig. 2. (Color online) Magnetic field dependence of magnetization in temperature intervals (a) 5–40 K and (b) 40–70 K. Inset of (a): forward M-H curves at 5 K. The straight line indicates the linear fitting done to find the amount of antiferromagnetic phase. Inset of (b): return M-H curves at 5 K. The straight line indicates the linear fitting done to find the amount of ferromagnetic phase.

it is seen that, when $H_c < H_w$, it leads to a lower magnetization value whereas when $H_c > H_w$, the magnetization value is higher, at the same warming field. These typical field-temperature induced transitions are best explained by the interplay of supercooling (H^*,T^*), superheating (H^{**},T^{**}) and kinetic arrest (H_K,T_K) bands, as described elaborately in reference [4]. Figures 1d and 1e show the field response magnetization with increasing magnetic field after cooling the compound to 5 K and 25 K in zero and at different fields. While cooling in different fields, different amounts of arrested phase results due to the interplay of (H_K,T_K) and (H^*,T^*) bands and de-arrest take place when (H_K,T_K) bands are approached in opposite sense, which is indicated by a sharp change in the value of magnetization, as magnetic field is increased. The graphs of these figures will be subsequently used to obtain magnetic field and temperature values, for tracing the various bands.

Further, the M-H curve of the compound also shows interesting features, resulting from the interplay of (H_K,T_K) and (H^*,T^*) bands. From Figure 2, a sharp slope change is observed in forward M-H curve (0 to H_{max}), indicating an AF-I to FM-M transition. The forward curve is not traced by the return one indicating irreversibility of the transition. From Figure 2a it is observed that the forward M-H curve shifts to lower field value with increasing temperature up to 40 K while for temperature higher than 40 K it shifts to higher field as seen from Figure 2b. The observed characteristics are very appealing as for normal cases the forward M-H curves shift to lower field with the enhancement in temperature. This anomalous behavior of M-H isotherm is explained later in Section 3.7.

3.2 Calculation of the transformed FM-M phase fraction owing to association among (H_K,T_K) and (H^*,T^*) bands

Hence in this compound it is observed that, different amounts of FM and AF fractions are present while cooling to lowest temperature in different fields and both of these fractions will contribute to magnetization at the given temperature and magnetic field. Hence, to calculate the correct amount of transformed FM-M phase fraction (f_T) we use the following equation:

$$M_{\text{measured}} = f_T(\alpha' H + M_o) + (1 - f_T)\,\alpha(T) H_c. \quad (1)$$

M_{measured} is the magnetization value at 5 K after cooling at the respective fields and its values are taken from the graph obtained from field-annealing graph at 5 K shown in Figure 1d. Here, (1–f_T) corresponds to the amount of AF-I phase in the compound. As the amount of AF-I fraction varies with field, a field dependent correction factor $\alpha(T)$ is introduced, which is constant at a particular temperature. The value of $\alpha(T)$ is obtained from the slope of the linear fit of the straight portion of forward M-H isotherms at 5 K (inset of Fig. 2a). Similarly, field dependent correction factor for FM-M fraction, α', is introduced in the equation for the FM phase. Its value is obtained from the slope of the linear fit of the straight portion of the return M-H curve (inset of Fig. 2b). The intercept of the above fitting gives the value of M_o. Using equation (1) it is found that cooling in 6, 5, 4, 3, 2 and 1 Tesla corresponds to 69.5%, 57.0%, 40.6%, 27.3%, 13.9% and 3.1% of transformed FM-M phase fraction, respectively. The above exercise is necessary as the percentage of transformed FM-M phase fraction will be helpful in finding various magnetic field and temperature points, which will be used in tracing out different regions of the bands in the H-T plane (in the calculation, temperature dependence of FM-M phase is not taken into account as it will introduce very minor correction (>1%); this conclusion is drawn from Figure 2, where it is observed that at high fields the value of magnetization changes insignificantly at different temperatures).

3.3 Kinetic Arrest (H_K,T_K) band of $Pr_{0.5}Ca_{0.5}Mn_{0.975}Al_{0.025}O_3$

The kinetic arrest band of the compound, traced out in H-T plane is shown in Figure 3. In the figure, seven lines are drawn to illustrate six arrested regions (viz. a, b, c, d, e, and f) of the compound. Each line is drawn by joining different magnetic fields and temperature points, corresponding to the same amount of transformed FM-M phase fraction, which is acquired by various CHUF protocols. Now the procedure for acquiring different magnetic field and temperature points, required for band tracing is described. Firstly, the open circular symbols are the magnetic field points obtained from the field annealing M-H graphs (shown in Figs. 1d and 1e) at the fixed temperatures. It is seen from the annealing graphs that with the increase in magnetic field, magnetization increases, with a sharp change in its value as (H_K,T_K) band is encountered, indicating the starting point of dearrest. Secondly, to crosscheck the above regions temperature points for fixed magnetic fields (represented by closed square points) are taken from field annealing M-T graphs of Figures 1a, 1b and 1c. Here the compound is field cooled

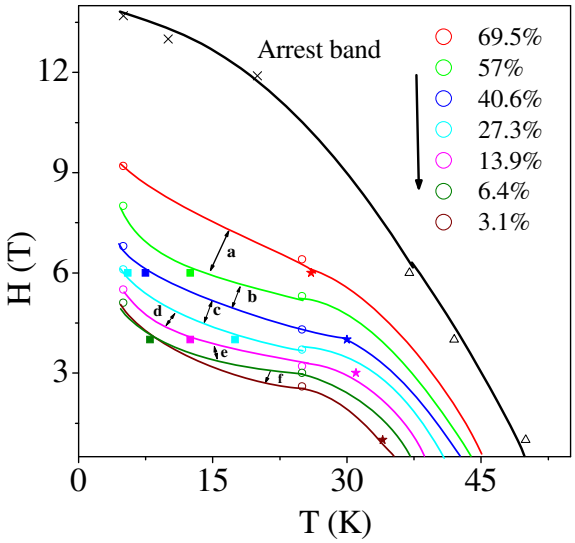

Fig. 3. (Color online) Kinetic arrest (H_K,T_K) band in the H-T phase diagrams for the compound $Pr_{0.5}Ca_{0.5}Mn_{0.975}Al_{0.025}O_3$.

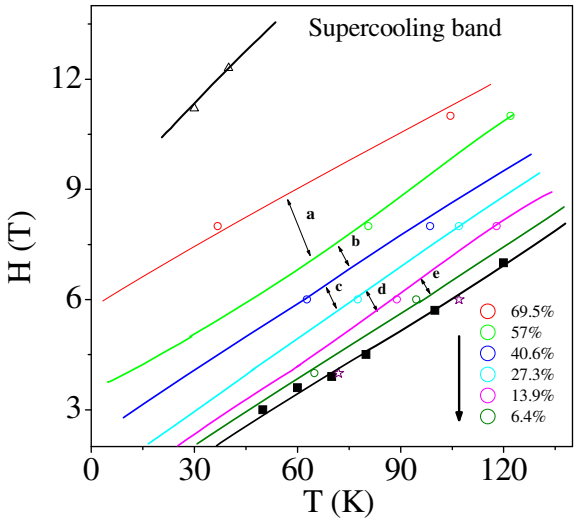

Fig. 4. (Color online) Supercooling (H^*,T^*) band in the H-T phase diagram for the compound $Pr_{0.5}Ca_{0.5}Mn_{0.975}Al_{0.025}O_3$.

to 5 K corresponding to the cooling field of Figure 1d for keeping the same amount of transformed FM-M phase fraction. Then the field is raised isothermally to warming field value and the temperature response of magnetization is noted, which shows a sharp change as (H_K,T_K) band is approached. Thus various dearrest points (temperature points) for each cooling field is obtained at fixed warming fields. These temperature points were found to lie exactly on corresponding (H_K,T_K) line constructed from the above-mentioned field annealing M-H graphs. Thirdly, the star points are obtained from the FCW curves (Figs. 1a, 1b and 1c) at different fields where an increase in magnetization (indicating dearrest point for respective transformed FM-M phase fraction) is observed. These points were also found to lie on corresponding (H_K,T_K) line. Finally, the open triangular symbols indicating end points of arrest band are obtained from the ZFC curve at different fields (Figs. 1a, 1b and 1c) where the increase in magnetization ceases. The high field magnetic field points (cross points) of the band are obtained from M-H isotherms where a full saturation (3.5 μ_B/(f.u.)) is achieved indicating a complete dearest of the AF-I phase to FM-M phase.

3.4 Supercooling (H^*,T^*) band of $Pr_{0.5}Ca_{0.5}Mn_{0.975}Al_{0.025}O_3$

The procedure for tracing the supercooling band of the compound is described in this section and the (H^*,T^*) band is shown in Figure 4. As observed from Figure 3, the role of the arrest band diminishes above 50 K and hence the slope change in forward M-H isotherms (AF-I to FM-M transformation) above 40 K is attributed to encountering of (H^*,T^*) band. The field for slope change from 40 K onwards is seen to increase with increasing temperature (Fig. 2b), indicating that supercooling band stretches to higher magnetic field at higher temperature. Therefore, for marking the (H^*,T^*) band, firstly, the magnetic field point of slope changes (obtained from forward M-H isotherms) are represented by closed squares in Figure 4. Secondly, the star points in the figure were obtained from FCC cycles at different fields where sharp increase in magnetization (as (H^*,T^*) band is encountered) is observed, also lie exactly on the line joining the magnetic field points from M-H isotherms. This shows that while cooling in field a conversion from AF-I to FM-M occurs on approaching the supercooling band. Thirdly, the high field magnetic field points (open triangles) of the band are obtained from M-H isotherms where a full saturation 3.5 μ_B/(f.u.) is achieved i.e. indicating the complete transformation to FM-M phase. Finally, the amount of FM phase at different temperatures is calculated from the FCC measurement done at different field using equation (1). Temperatures corresponding to different values of transformed FM-M phase fraction were noted. Temperature points (shown by open circles) of equivalent values of transformed FM-M phase fraction at various cooling fields were joined, resulting in tracing of corresponding regions in (H^*,T^*) band, which are already identified in the (H_K,T_K) band.

3.5 Superheating (H^{**},T^{**}) band of $Pr_{0.5}Ca_{0.5}Mn_{0.975}Al_{0.025}O_3$

Similar to the other two bands, the process of marking of superheating band (Fig. 5) of the compound is described in this section. Firstly, the star points of band are the magnetic field points obtained from return M-H isotherms (Fig. 2) where a sharp decrease in magnetization is observed. As field is reduced, transformation from FM-M to AF-I happens on encountering the superheating band. The

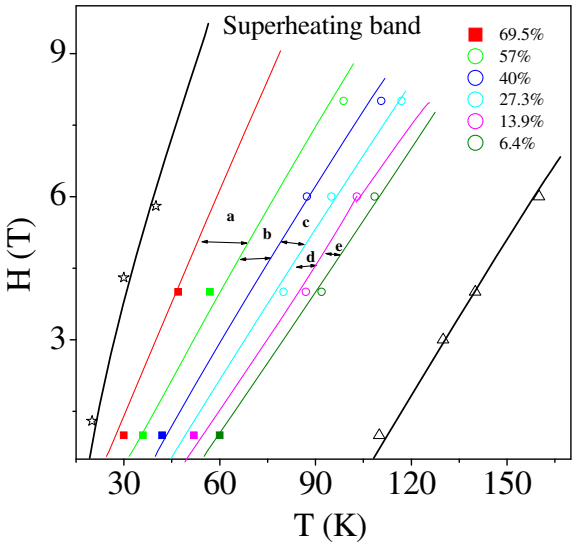

Fig. 5. (Color online) Superheating (H^{**},T^{**}) band in the H-T phase diagram for the compound $Pr_{0.5}Ca_{0.5}Mn_{0.975}Al_{0.025}O_3$.

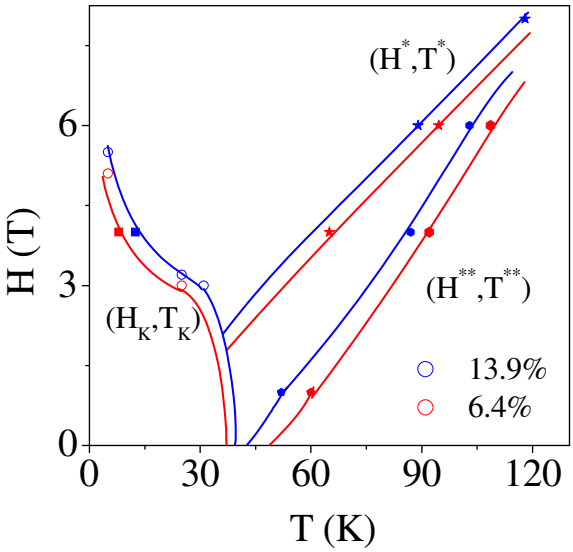

Fig. 6. (Color online) Two spinodal lines of all the three bands showing anti-correlation among the (H_K,T_K) and (H^*,T^*), (H^{**},T^{**}) bands and correlation among latter two bands.

value of these magnetic field points decreases as temperature is lowered, indicating (H^{**},T^{**}) band monotonically decreases with decrease in temperature. Secondly, the high temperature points (shown by open triangle) of (H^{**},T^{**}) band were obtained from the FCW curve where it merges with the FCC curve (Figs. 1a, 1b and 1c) indicating the end points of the band. Thirdly, for $H_w > H_c$, the low temperature FM-M phase transforms to AF-I on approaching the superheating band with increasing temperature. Since, cooling in various fields results in different amounts of transformed FM-M phase fraction; corresponding temperature points at fixed warming field (4 T and 1 T) are identified from Figures 1a and 1b where a sharp decrease in magnetization is observed in the M-T curve for $H_w > H_c$. These points for different transformed FM-M phase fraction are represented by closed squares in H-T plane. Finally, calculations similar to that of FCC cycle were done for FCW cycle for identifying different regions of the superheating band. Temperature points (open circles) of equivalent values of transformed FM-M phase fraction for different warming field are joined, leading to tracing of corresponding regions in (H^{**},T^{**}) band, which are already identified in other two bands.

3.6 H-T phase diagram of $Pr_{0.5}Ca_{0.5}Mn_{0.975}Al_{0.025}O_3$

Figure 6 represents the two spinodal lines of all the three bands. These lines are sketched using points corresponding to two values of the calculated transformed FM-M phase fraction. This picture will help to visualize the nature of all the three bands in the same graph. From the graph it is clearly seen that the slope of both supercooling/heating is similar indicating that correlation exists between the two bands. However the slope of the arrest and the supercooling/heating band is dissimilar indicating an anticorrelation between them.

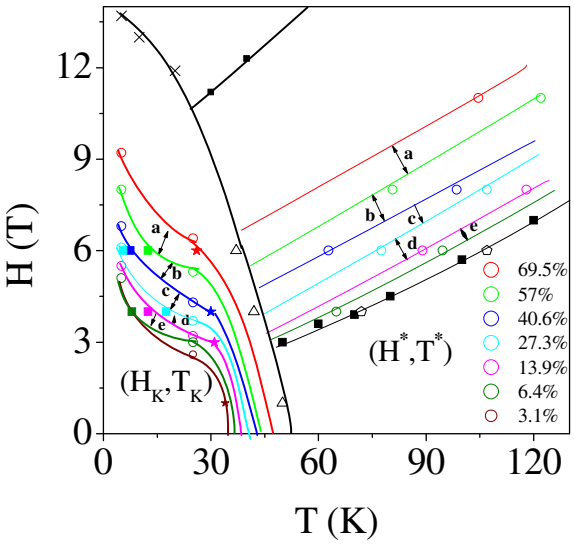

Fig. 7. (Color online) Kinetic arrest and supercooling band in the H-T plane for the compound $Pr_{0.5}Ca_{0.5}Mn_{0.975}Al_{0.025}O_3$.

Figure 7 shows the total (H^*,T^*) and (H_K,T_K) arrest band. From the figure it is inferred that a complete transformation of the AF-I to FM-M phase on crossing the (H^*,T^*) band occurs when the compound is cooled in a field above 10 Tesla. The inverted triangular region between (H^*,T^*) and (H_K,T_K) band is a stable FM region. In this region the magnetization of the compound remains unchanged even if magnetic field or temperature is varied. Cooling the compound in lower field results in coexistence of partially transformed FM-M phase and remaining arrested AF-I phase up to the lowest temperature due to the interplay of the arrest and the supercooled band.

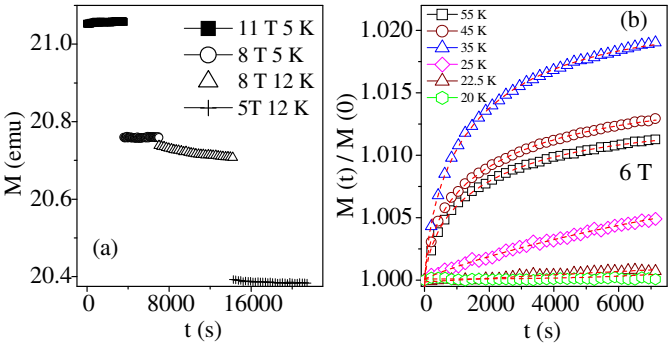

Fig. 8. (Color online) (a) Time dependence of magnetization for 1 h at 5 K after cooling in 11 Tesla. The magnetic field is reduced to 8 Tesla and the dependence is noted for an hour. The temperature is increased to 12 K and the dependence noted for 2 h. The magnetic field is reduced to 5 Tesla and dependence is noted for 2 h. (b) Time dependence of M (t) at constant field. Every time the compound is cooled in 6 Tesla from 200 K to the measurement temperature and the time dependence is noted for 2 h. The growth in magnetization increases up to 35 K and on further reduction in temperature the growth ceases. Dashed lines are fits using equation (2).

3.7 Investigation of the stable ferromagnetic region and anomalous features of M-H isotherms

To probe the stable FM region stated above, the compound has been cooled in 11 Tesla to 5 K and thermoremanent magnetization (TRM) is measured for an hour. No change in magnetization is observed with time, indicating a stable FM region. For further confirmation, field is reduced to 8 Tesla and TRM is measured for an hour (Fig. 8a). Then temperature is increased up to 12 K and time variation of magnetization is noted for 2 h. Field is further reduced to 5 Tesla and TRM is measured for another 2 h. For all cases of temperature and field cycling magnetization remains unchanged with time indicating the stable FM remains unaffected against any perturbation (it may be noted that the slight changes in the values of M (>0.1%) arise due to the contribution of the sample holder). However, a growth in magnetization is observed with time under same situation when cooled in lower fields, indicating that cooling in lower field results in a metastable state at the same temperature (Fig. 4a of Ref. [4]).

The anomalous features of M-H isotherms described earlier (Fig. 2) is explained in this paragraph. From Figure 3 it is clear that (H_K,T_K) band in the compound plays a significant role up to 40 K. The arrested AF-I phase gets dearrested and transforms into FM-M phase on encountering the (H_K,T_K) band. The field value for which the slope change occurs in forward curve decreases with the increase in temperature, as the arrest band tends to zero with increasing temperature. Hence the forward M-H isotherm shifts monotonically to lower field values with rising temperature. Above 40 K, (H^*,T^*) band dominates the (H_K,T_K) band and the slope change in M-H curves occurs on encountering the (H^*,T^*) band instead of (H_K,T_K) band, effecting the transformation of AF-I to FM-M phase. From Figure 4, it is seen that the slope of (H^*,T^*) band is positive. Hence the field point of slope change of the M-H curves increases with temperature, as (H^*,T^*) band tends to increase with raising temperature. This results in the shifting of forward M-H curve to higher field value with increasing temperature.

Table 1. Values of fitting parameters M', M_1, n and τ of equation (2) for TDM's at different temperatures.

T(K)	M'(emu)	M_1(emu)	n	$\tau \times 10^3$
55	0.176(1)	13.530(1)	0.592(6)	1.9 ± 0.03
45	0.221(1)	14.204(1)	0.543(7)	2.1 ± 0.03
35	0.315(2)	14.617(2)	0.606(5)	1.6 ± 0.02
25	0.172(2)	14.540(2)	0.903(30)	16 ± 5
22.5	0.0005(4)	14.480(2)	0.999(177)	41 ± 120

3.8 Comparing the metastabilities of supercooling and arrested kinetics through time decay

Finally, to show that the supercooled phase is different from the kinetic arrest phase, time dependent magnetization (TDM) measurement is done at different temperatures after cooling the compound from 200 K in 6 Tesla (Fig. 8b). The temperatures chosen are based on the band diagrams in Figures 3 and 4. It is seen that the growth of magnetization is more at 45 K than 55 K and it increases further as temperature is reduced to 35 K. This indicates that the supercooled band dominate the arrest band in the above temperature region for the given field. As the temperature is reduced further the role of arrest band becomes important and the increase in magnetization is reduced as seen for 25 K. No significant time dependence is observed on further reduction in temperature. This indicates that arrest band totally dominates the proceedings resulting in an increase of relaxation time. For quantitative analysis of the TDM data, the curves are fitted (solid line in Fig. 8b) by the stretched exponential function with a constant. The functional form is represented as

$$M(t) = M_1 - M' \exp[-(t/\tau)^n], \qquad (2)$$

where the parameters M' and M_1 are constants, τ is the relaxation time and n is an exponent. The necessity to supplement the stretched exponential with a substantial baseline term M_1, which approximates up to 90–95% of the signal is consistent with similar measurements in other systems where there is phase coexistence [19]. Satisfactory fit with χ^2 (goodness of fit) $\approx 10^{-8}$ is obtained for temperatures 35–55 K. The fitting parameters using equation (2) are summarized in Table 1. From the table it is clearly seen that the relaxation time decreases when temperatures where TDM's are measured lie in (H^*,T^*) band (with a minor anomaly at 45 K). At 25 K, as the system enters the (H_K,T_K) band relaxation time is seen to increase. On cooling, the relaxation time further increases. The error bar corresponding to the relaxation time is significant indicating that equation (2) do not give a good

fit. This also verifies the fact that a kinetically arrested glassy state cannot reach an equilibrium value over the experimental time scales. For 20 K the error bar for the corresponding fitting parameters is more than the values (and hence is not summarized in Tab. 1). The values of M' and M_1 systematically increase up to 35 K and decrease below as the temperature is reduced further, signifying that a changeover in region has taken place. Similarly, the value of n changing drastically below 35 K also verifies the above statement.

4 Conclusion

In summary, H-T phase diagram of $Pr_{0.5}Ca_{0.5}Mn_{0.975}Al_{0.025}O_3$ compound consisting of (H_K,T_K), (H^*,T^*) and (H^{**},T^{**}) bands have been traced out from various experimental data. It has been shown that disorder in a system results in the formation of (H_K,T_K) band, similar to (H^*,T^*) and (H^*,T^*) band. Quantitatively, it is shown that the (H_K,T_K) band is anticorrelated with the (H^*,T^*), (H^{**},T^{**}) bands while the later two are correlated. The H-T phase diagram obtained is used to explain the observed interesting behavior of M-H isotherms. A stable ferromagnetic region is identified in H-T plane which remains unperturbed with magnetic field or temperature variation. From quantitative analysis of TDM measurements, it is seen that the supercooled state is different from a kinetically arrested state.

References

1. M.K. Chattopadhyay et al., Phys. Rev. B **72**, 180401(R) (2005)
2. K. Kumar et al., Phys. Rev. B **73**, 184435 (2006)
3. R. Rawat et al., J. Phys.: Condens. Matter **19**, 256211 (2007)
4. A. Banerjee et al., Phys. Rev. B **74**, 224445 (2006)
5. W. Wu et al., Nat. Mater. **5**, 881 (2006)
6. S.B. Roy et al., Phys. Rev. B **74**, 012403 (2006)
7. S.B. Roy et al., Phys. Rev. B **75**, 184410 (2007)
8. P. Chaddah et al., Phys. Rev. B **77**, 100402(R) (2008) and references therein
9. A. Banerjee et al., Phys. Rev. B **79**, 212403 (2009) and references therein
10. A. Banerjee et al., J. Phys.: Condens. Matter **20**, 255245 (2008)
11. A. Banerjee et al., J. Phys.: Condens. Matter **21**, 026002 (2009)
12. J.D. Moore et al., J. Phys.: Condens. Matter **20**, 465212 (2008)
13. M.H. Phan et al., Sol. State Commun. **150**, 341 (2010)
14. J.A. Mydosh, *Spin glasses* (Taylor and Francis, London, 1992)
15. S.B. Roy, M.K. Chattopadhyay, Phys. Rev. B **79**, 052407 (2009)
16. S.B. Roy, P. Chaddah, Phase Transit. **77**, 767 (2004)
17. S.B. Roy et al., Phys. Rev. Lett. **92**, 147203 (2004) and references therein
18. M.A. Manekar et al., Phys. Rev. B. **64**, 104416 (2001)
19. D. Li et al., Phys. Rev. B. **49**, 9601 (1994)